Polarization measurements of the Lyman-α_1 x-ray emission lines of hydrogenlike Ar^{17+} and Fe^{25+} at high electron-impact energies

D. L. Robbins,[1] P. Beiersdorfer,[2] A. Ya. Faenov,[3] T. A. Pikuz,[3] D. B. Thorn,[2] H. Chen,[2] K. J. Reed,[2] A. J. Smith,[1] K. R. Boyce,[4] G. V. Brown,[4] R. L. Kelley,[4] C. A. Kilbourne,[4] and F. S. Porter[4]

[1]*Department of Physics, Morehouse College, Atlanta, Georgia 30314, USA*

[2]*University of California Lawrence Livermore National Laboratory, Livermore, California 94550, USA*

[3]*Multicharged Ions Spectra Data Center of VNIIFTRI, Mendeleevo, Moscow region, 141570 Russia*

[4]*NASA Goddard Space Flight Center, Greenbelt, Maryland 20771, USA*

(Received 8 February 2006; revised manuscript received 20 May 2006; published 9 August 2006)

We have measured the polarization of the $2p_{3/2} \rightarrow 1s_{1/2}$ Lyman-α_1 x-ray line of hydrogenlike Ar^{17+} and Fe^{25+} at electron-impact energies ranging from 7 to 25 threshold units. The highly charged argon and iron ions were produced using the Lawrence Livermore National Laboratory SuperEBIT electron beam ion trap. A combination of two crystal spectrometers and a microcalorimeter were used to record the Lyman-α x-ray emission of Ar^{17+} and Fe^{25+} and to infer the polarization of the Lyman-α_1 line. Our results show a systematic discrepancy with the predictions of distorted-wave calculations.

DOI: 10.1103/PhysRevA.74.022713 PACS number(s): 34.80.Kw, 32.30.Rj, 52.27.Ny

I. INTRODUCTION

Polarization spectroscopy has the potential of being used as a plasma diagnostic tool [1–3]. Polarized x rays emitted from plasmas hint at the presence of electron beams, hence at an anisotropic electrons distribution function. This innovative diagnostic has been applied successfully to plasmas produced by lasers [4], vacuum sparks [5], electron beam ion traps [6], and *Z* pinches [7,8]. Testing the accuracy of theoretical predictions in a controlled experiment is of importance for assessing the accuracy of the diagnostic. Nakamura *et al.* previously reported the polarization of the Lyman-α_1 line in hydrogenlike titanium as a function of electron-impact energy [9]. Their results showed an unexplained systematic discrepancy with the predictions provided by fully relativistic distorted-wave calculations. The discrepancy between measured and predicted polarization is the catalyst for the present study. The discrepancy they found is especially intriguing because studies of the *K*-shell x-ray emission lines of various heliumlike and lithiumlike ions Fe^{24+}, Ti^{20+}, Sc^{19+}, Fe^{23+}, and Ti^{19+} [10–13], seem to agree well with theory. Good agreement with theory was also found in a recent measurement of heliumlike and lithiumlike sulfur [14], which was done at electron-impact energies up to 60 threshold units. Moreover, measurements of the polarization of certain lines in neonlike barium appear to agree with theory [15]. A further investigation of the polarization of Lyman-α_1 lines of highly charged ions therefore appears warranted.

In this paper we report the polarization of Lyman-α_1 x-ray emission line in hydrogenlike Ar^{17+} at two electron-impact energies (30 and 84 keV), as well as a measurement for hydrogenlike Fe^{25+} at electron impact energies of 30 and 120 keV. Our results are compared to the results of fully relativistic distorted-wave calculations. The predicted polarization values tend to be larger than the measured results, confirming the trend reported by Nakamura *et al.* [9] for Ti^{21+}.

II. MEASUREMENT

The hydrogenlike argon and iron ions were produced using the Livermore SuperEBIT electron beam ion trap [16]. Neutral argon and iron atoms were introduced into the electron beam ion trap apparatus by way of a gas injector. SuperEBIT contains a quasi-mono-energetic electron beam magnetically compressed to ~ 60 μm diameter which both radially confines and electronically excites the trapped ions. Due to the excitation by directional electron collisions, the magnetic sublevels are unevenly populated resulting in the emission of polarized x rays.

The high-resolution crystal spectrometers we employed to measure the x-ray emission are sensitive to polarization [17,18]. The intensity of the emitted x rays observed by a crystal spectrometers can be expressed as

$$I^{\text{observed}} = I_{\parallel} R_{\parallel} + I_{\perp} R_{\perp}, \tag{1}$$

where $I_{\parallel}$ and $I_{\perp}$ denote intensity of the radiation emitted parallel and perpendicular to the electron beam propagation, respectively. $R_{\parallel}$ and $R_{\perp}$ represent the integrated crystal reflectivities for x-ray emission polarized parallel and perpendicular to the plane of dispersion, respectively. Integrated crystal reflectivities are usually tabulated as the ratio $\mathcal{R} = R_{\parallel}/R_{\perp}$. For a perfect crystal the integrated reflectivity ratio varies as a function of $|\cos(2\theta_B)|$, while that of a mosaic crystal varies as a function of $\cos^2(2\theta_B)$, where θ_B denotes the Bragg angle [19].

All of the spectrometers and detectors used to record x-ray emission lines from the Livermore EBIT are placed at an observation angle 90° relative to the electron beam. The polarization at this angle is defined as

$$P \equiv \frac{I_{\parallel} - I_{\perp}}{I_{\parallel} + I_{\perp}}. \tag{2}$$

By proper selection of the crystal we can use a crystal spectrometer to infer the polarization of a particular x-ray emission line. When measuring the polarization of Lyman-α_1 in hydrogenlike Fe^{25+} we used a crystal spectrometer arranged in the von Hámos geometry [16] concurrently with a high-resolution x-ray spectrometer (XRS) microcalorimeter [20]. The von Hámos-type crystal spectrometer was equipped with

a Si(400) crystal, which had a lattice spacing $2d=2.715$ Å, resulting in a Bragg angle of $\theta_B=40.91°$ for the transition of interest. The dispersion plane of the von Hámos–type crystal spectrometer was perpendicular to the electron beam propagation. Si(400) is a perfect crystal, and its integrated crystal reflectivity ratio varies as $|\cos(2\theta_B)|$. At the Bragg angle of the measurement $\mathcal{R}_{\mathrm{Si400}}$ is ~0.13. Therefore, the von Hámos crystal spectrometer preferentially reflects the $I_{\|}$ component in Eq. (1) while absorbing most of $I_{\perp}$. On the other hand, the XRS microcalorimeter records both polarization components with equal (approximately unity) quantum efficiency. The intensity observed by the XRS can be approximated as

$$I_{\mathrm{XRS}}^{\mathrm{observed}} = I_{\|} + I_{\perp}. \tag{3}$$

The XRS has a resolution of ~8 eV compared to ~1.3 eV for the von Hámos crystal spectrometer. Both instruments thus resolve Lyman-α_1 and Lyman-α_2 in hydrogenlike Fe^{25+}, which are separated by ~21 eV. Figure 1 shows the spectra obtained by both the XRS and the von Hámos crystal spectrometer for the hydrogenlike Fe^{25+} Lyman-α emission at the two energies of our study.

The Lyman-α_2 transition $(2p_{1/2} \rightarrow 1s_{1/2})$ observed at 6952 eV is intrinsically unpolarized, and is thus used here for cross-normalization between the two instruments. Applying this normalization with some algebraic manipulation of Eq. (1)–(3), we can derive an expression for the polarization of Lyman-α_1

$$P_{\text{Ly-}\alpha 1} = \frac{(\mathcal{R}+1)}{(\mathcal{R}-1)} \frac{\left[\left(\frac{I_{\text{Ly-}\alpha 1}}{I_{\text{Ly-}\alpha 2}}\right)_{\mathrm{XRS}} - \left(\frac{I_{\text{Ly-}\alpha 1}}{I_{\text{Ly-}\alpha 2}}\right)_{\mathrm{VH}}\right]}{\left(\frac{I_{\text{Ly-}\alpha 1}}{I_{\text{Ly-}\alpha 2}}\right)_{\mathrm{XRS}}}, \tag{4}$$

where $\mathcal{R}$ denotes the integrated reflectivity ratio for Si(400) and $(I_{\text{Ly-}\alpha 1}/I_{\text{Ly-}\alpha 2})$ is the measured line intensity ratio observed by either the XRS or the von Hámos crystal spectrometer. Equation (4) is the result of applying the "two crystal spectrometer technique" to infer the polarization of x-ray line emission [10,14].

Given the simplicity of the hydrogenlike Lyman-α spectrum, the combination of spectral data provided by a crystal spectrometer and "good" theoretical predictions of the total effective excitation cross sections for Lyman-α_1 and Lyman-α_2 should be sufficient to infer the polarization of Lyman-α_1. This technique, dubbed here as the "one-crystal method," was used in Ref. [9] to infer the polarization of Lyman-α_1 in Ti^{21+}. This technique is also employed here, and it appears to give the same answer as the two crystal spectrometer technique. The equation used to infer the polarization using the one-crystal method is

$$P_{\text{Lyman-}\alpha 1} = \frac{3 - 3\mathcal{R} - 3\left|(1+\mathcal{R})\frac{I^{\mathrm{measured}}}{I^{\mathrm{theory}}}\right|}{-\frac{I^{\mathrm{measured}}}{I^{\mathrm{theory}}} - 3 + 3\mathcal{R}}. \tag{5}$$

Equation (5) is equivalent to Eq. (7) in Ref. [9], where $\mathcal{R}$, I^{measured}, and I^{theory} denote the integrated crystal reflectivity ratio, the ratio of the measured intensity of Lyman-α_1 to Lyman-α_2 $(I^{\text{Ly-}\alpha 1}/I^{\text{Ly-}\alpha 2})$, and the ratio of the effective excitation cross sections of Lyman-α_1 to Lyman-α_2 $(\langle\sigma^{\text{Ly-}\alpha 1}\rangle/\langle\sigma^{\text{Ly-}\alpha 2}\rangle)$, respectively.

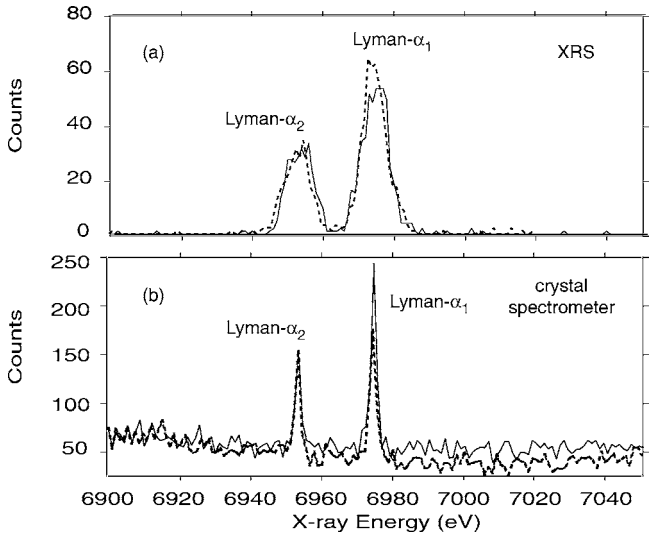

FIG. 1. Lyman-α emission spectra of Fe^{25+} obtained with (a) the XRS microcalorimeter and (b) the von Hámos crystal spectrometer. Spectra taken concurrently at an electron beam energy of 30 keV are shown as solid lines; those recorded at an electron beam energy of 120 keV are shown as dashed lines. The exposure time was chosen such that the intensity of Lyman-α_2 was the same in each case.

For hydrogenlike Ar^{17+}, Lyman-α_1, and Lyman-α_2 are separated by only 4 eV. Hence, the XRS cannot resolve these two transitions, therefore only one crystal spectrometer is used here to infer the polarization of Lyman-α_1 for Ar^{17+}. For the lower energy measurement taken at 30 keV, we employed a compact spherical crystal spectrometer arranged in the Johann geometry [18]. The measured spectrum is shown in Fig. 2. The spherical crystal spectrometer used a quartz $(11\bar{2}0)$ crystal, which has a $2d$ spacing of 4.912 Å, resulting in a Bragg angle $\theta_B=49°$ for the Lyman-α transitions for Ar^{17+}. Its dispersion plane is parallel to the electron beam propagation. A charge-couple device (CCD) was used with

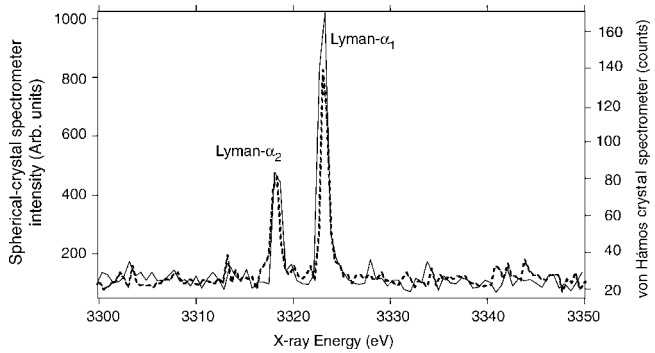

FIG. 2. Lyman-α emission spectrum of Ar^{17+} obtained with the spherical crystal spectrometer at an electron beam energy of 30 keV (solid line) and with the von Hámos crystal spectrometer at an electron beam energy of 84 keV (dashed line). The scales have been adjusted by equalize the height of Lyman-α_2 for each measurement.

this spectrometer for x-ray detection. For the high energy measurement taken at 84 keV, we used the von Hámos crystal spectrometer equipped with a Si(111) crystal. This crystal had a $2d$ spacing of 6.271 Å resulting in a Bragg angle of $\theta_B=36.5°$ for the Lyman-α transitions for Ar^{17+}. The measured spectrum is also shown in Fig. 2. The von Hámos crystal spectrometer used a position-sensitive proportional counter for x-ray detection [21]. Since both spectrometers have Bragg angles fairly close to 45°, the integrated crystal reflectivity ratio for both are expected to be small. Using $\mathcal{R}$ values tabulated by Henke *et al.* [19], $\mathcal{R}_{\mathrm{Si111}}\sim 0.15$ and $\mathcal{R}_{\mathrm{quartz}}\sim 0.14$.

III. THEORY

Using the distorted-wave code developed by Zhang, Sampson, and Clark [22], we calculated the magnetic sublevel cross sections for Lyman-α_1, Lyman-α_2, and the $2s_{1/2}\rightarrow 1s_{1/2}$ $M1$ transition, which blends with Lyman-α_2, for both hydrogenlike Ar^{17+} and Fe^{25+} at electron impact energies ranging from 5 to 25 threshold units. The same code was used in Ref. [9] for the comparison with the measurements, but only values up to 5 times threshold were available at the time. The theoretical results are used to estimate the polarization as well as the ratio of the effective cross sections needed in Eq. (5). The calculated magnetic sublevel cross sections are related to the polarization by the following expression:

$$P=\frac{3(\sigma_{1/2}-\sigma_{3/2})}{3\sigma_{3/2}+5\sigma_{1/2}}, \tag{6}$$

where $\sigma_{1/2}$ and $\sigma_{3/2}$ denote the cross sections for electron impact excitation from the ground level to the $m=1/2$ and $3/2$ magnetic sublevels for the $2p_{3/2}\rightarrow 1s_{1/2}$ Lyman-α_1 transition. Figures 3(a) and 3(b) show the total cross sections for Lyman-α_1, Lyman-α_2, and the $M1$ transition for both hydrogenlike Ar^{17+} and Fe^{25+} as a function of electron impact energy, respectively. The polarization values predicted by these calculations for argon and iron, as well as for titanium, are nearly identical when expressed in threshold units. The result is shown in Fig. 4.

IV. RESULTS, DISCUSSION, AND CONCLUSION

Each pair of Lyman-α lines was fitted with Gaussian profiles constrained to the same width. The measured intensities are then used in Eqs. (4) or (5) to infer the polarization of Lyman-α_1. Here, particularly for hydrogenlike Fe^{25+}, we used the two-spectrometer method in which all of the parameters listed in Eq. (5) are determined empirically (excluding the integrated reflectivity ratio $\mathcal{R}$). The measured polarization values are summarized and compared to theory in Table I. The inferred value employing the one-crystal method are $P=+0.05\pm 0.01$ at 30 keV and $P=-0.22\pm 0.05$ at 120 keV for Lyman-α_1 in Fe^{25+}. These values agree well the results obtained using the two-spectrometer method, which are $P=0.07\pm 0.03$ and $P=-0.24\pm 0.11$, respectively. The error bars in all cases are dominated by the statistical error, and were obtained by taking the quadrature sum of the statistical error and the error due to the uncertainty of the integrated crystal reflectivity ratios.

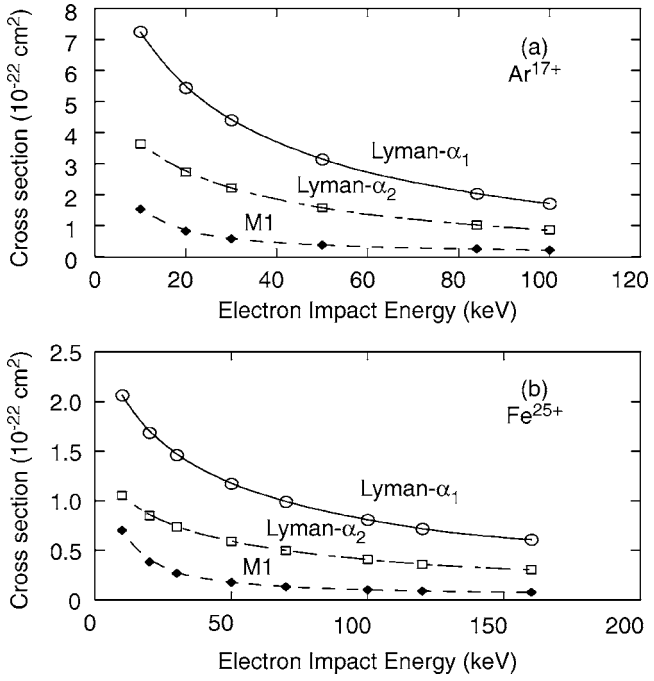

FIG. 3. Total excitation cross sections predicted by distorted-wave calculations for the Lyman-α_1, Lyman-α_2, and $M1$ transition due to electron impact excitation for (a) hydrogenlike Ar^{17+} and (b) hydrogenlike Fe^{25+}.

The four measured polarization values for the Lyman-α_1 transition in Fe^{25+}, using both the two crystal spectrometer and the one-crystal technique, are compared in Fig. 4 to the predictions of the distorted-wave calculations. Here, we also show the measured polarization values for the Lyman-α_1 transition in Ar^{17+}, as well as those reported earlier by Nakamura *et al.* for Lyman-α_1 in hydrogenlike titanium [9]. A common trend is observed: The polarization values predicted

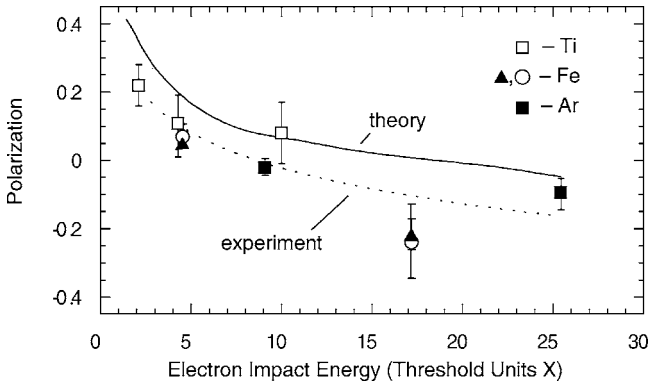

FIG. 4. Measured polarization of the Lyman-α_1 emission line of Fe^{25+}, Ar^{17+}, and Ti^{21+} compared to the predictions from distorted-wave calculations (solid curve). All electron-beam energies values are plotted in threshold units (X). The dotted curve represents a fit of the measured polarization values. In the case of iron, results obtained with the one-crystal method are shown as solid triangles; results obtained with the two-spectrometer technique are given as open circles.

TABLE I. Polarization measurements for Lyman-α_1 of Fe^{25+} and Ar^{17+} compared to the predictions of distorted-wave calculations.

Beam energy (keV)	$P_{\text{Ly-}\alpha 1}(Fe^{25+})$			$P_{\text{Ly-}\alpha 1}(Ar^{17+})$	
	measured[a]	measured[b]	distorted wave	measured[b]	distorted wave
30	+0.071±0.034	+0.051±0.011	+0.194	−0.019+0.025	+0.072
84				−0.099±0.045	−0.049
120	−0.236±0.109	−0.217±0.045	+0.007		

[a]Polarization measurements were obtained using the "two crystal spectrometer method."
[b]Polarization measurements were obtained using the "one-crystal method."

by the distorted-wave calculations are systematically larger than the measurements. In fact, a fit through the measured values shown as a dashed curve in Fig. 4 reveals a general reduction of the polarization compared to theory by $\Delta P \approx 0.1$.

Several possible contributions to this discrepancy with theory have been considered. An immediate concern is the unresolved magnetic dipole transition ($M1$) which overlaps with the unpolarized Lyman-α_2 transition used for normalization. Similarly to the Lyman-α_2, the upper level of $M1$ line has a total angular momentum of 1/2, so it, too, is intrinsically unpolarized. The $M1$ transition contributes to the intensity of Lyman-α_2. We must account for this contribution in order to gauge its affect on the inferred polarization of Lyman-α_1. The branching ratio for the $M1$ line in Fe^{25+} has been predicted to be ~10% [23]. The ratio is even less in the case of Ar^{17+}. Combining this with the calculated electron impact excitation cross sections for the $M1$ line at the relevant beam energies, we were able to correct for its intensity contribution to Lyman-α_2. Taking this effect into account shows that the associated corrections have little effect on the inferred polarization measurements. For example, we calculate that the $M1$ line only contributes ~4% to the intensity of Lyman-α_2 at 30 keV and ~2% at 120 keV for hydrogenlike Fe^{25+}. For Ar^{17+}, where the branching ratio leading to the production of the $M1$ line is yet smaller, the total contribution is negligible.

The transverse motion of the electron beam ion trap, charge exchange (CX), and possible incorrect integrated reflectivity ratio values ($\mathcal{R}$) have also been considered as possibilities for the discrepancy. The transverse motion of the electron beam has been well studied and measured in previous experiments [6,24]. This component, if dominant, would depolarized the x-ray lines emitted from the ions trapped in EBIT, but the transverse beam component of SuperEBIT is relatively small and thus has a negligible effect on the emitted polarized x rays specifically at high beam energies [6,24]. We have also checked the effect of CX. Bare Fe and Ar ions in the electron beam ion trap can grab electrons from neutral atoms made available by the ambient gas load [25–27]. Charge transfer can populate the $2p$ level of the hydrogenlike ions and the transferred electron can radiate to the ground state via the Lyman-α_1 transition. Since the level is not populated by the directional electron beam, the x rays emitted due to CX are not polarized. We were able to measure the x rays due to CX by switching the electron beam off, i.e., by utilizing the magnetic trapping mode [12]. The XRS microcalorimeter was synchronized with the EBIT timing pattern, and we were therefore able to distinguish between x rays emitted when the beam was either on or off. We found that the number of x rays due to CX (beam off) was less than 2% of the number of x rays produced by electron impact excitation and CX (beam on). CX is thus deemed negligible.

Since predicted integrated reflectivity ratios are used here, errors due to possible incorrect $\mathcal{R}$ values are a concern. Although calculated integrated reflectivity ratios have been shown to be quite accurate [11,19], defects unique to a given crystal my may cause $\mathcal{R}$ to deviate from the predicted value, even for ideal crystals. We have made an attempt to include the predictions of $\mathcal{R}$ in our error analysis. This was done by recalculating the polarization at $\theta_B \pm 5°$, giving us an approximated upper and lower limit for predicted $\mathcal{R}$ values. Nakamura *et al.* [9] qualitatively investigated $\mathcal{R}$ for their crystal, and found that it matched the predicted value given by Henke *et al.* [19]. Given that we used three different crystal spectrometers in this study, we would not expect all three crystals to be defective. We conclude that predicted integrated reflectivity ratios are likely not the source of this discrepancy.

In conclusion the polarization of Lyman-α_1 of both hydrogenlike Fe^{25+} and Ar^{17+} have been measured at two electron impact energies well above their respective thresholds. The measured polarization values do not agree with the predictions of distorted-wave calculations, confirming a trend set by the earlier measurements [9] of Ti^{21+}. Additional studies both theoretical and experimental are needed to further understand the source of this discrepancy.

ACKNOWLEDGMENTS

We gratefully acknowledge the support by the Lawrence Livermore National Laboratory Research Collaborations Programs for Historically Black Colleges and Universities and Minority Institutions. This work was performed under the auspices of the U.S. Department of Energy by Lawrence Livermore National Laboratory under Contract No. W-7405-ENG-48 and by Morehouse College under Contract No. DE-FG02-98ER14877. P.B., A.F., and T.P. gratefully acknowledge support from NATO Collaborative Linkage Grant No. PST.CLG.97889.

[1] M. K. Inal, and J. Dubau, J. Phys. B **20**, 4221 (1987).
[2] E. Haug, Sol. Phys. **71**, 77 (1981).
[3] S. A. Kazantsev and J.-C. Henoux, *Plasma Polarization Spectroscopy of Ionized Gases* (Kluwer Academic Publishers, Dordrecht, 1995).
[4] J. C. Kieffer, J. P. Matte, M. Chaker, Y. Beaudoin, C. Y. Chien, S. Coe, G. Mourou, J. Dubau, and M. K. Inal, Phys. Rev. E **48**, 4648 (1993).
[5] R. Beier, C. Bachmann, and R. Burhenn, J. Phys. D **14**, 643 (1981).
[6] P. Beiersdorfer and M. Slater, Phys. Rev. E **64**, 066408 (2001).
[7] A. S. Shlyaptseva, S. B. Hansen, V. L. Kantsyrev, B. S. Bauer, D. A. Fedin, N. Ouart, S. A. Kazantsev, A. G. Petrashen, and U. I. Safronova, Rev. Sci. Instrum. **72**, 1241 (2001).
[8] A. S. Shlyaptseva, V. L. Kantsyrev, N. Ouart, D. Fedin, S. Hamasha, and S. Hansen, in Laser-Generated and Other Laboratory X-Ray and EUV Sources, Optics, Applications, Proc. SPIE **5196**, 16 (2003).
[9] N. Nakamura, D. Kato, N. Miura, T. Nakahara, and S. Ohtani, Phys. Rev. A **63**, 024501 (2001).
[10] J. R. Henderson, P. Beiersdorfer, C. L. Bennett, S. Chantrenne, D. A. Knapp, R. E. Marrs, M. B. Schneider, K. L. Wong, G. A. Doschek, J. F. Seely, C. M. Brown, R. E. LaVilla, J. Dubau, and M. A. Levine, Phys. Rev. Lett. **65**, 705 (1990).
[11] P. Beiersdorfer, D. A. Vogel, K. J. Reed, V. Decaux, J. H. Scofield, K. Widmann, G. Hölzer, E. Förster, O. Wehrhan, D. W. Savin, and L. Schweikhard, Phys. Rev. A **53**, 3974 (1996).
[12] P. Beiersdorfer, J. Crespo López-Urrutia, V. Decaux, K. Widmann, and P. Neil, Rev. Sci. Instrum. **68**, 1073 (1997).
[13] P. Beiersdorfer, G. Brown, S. Utter, P. Neil, K. J. Reed, A. J. Smith, and R. S. Thoe, Phys. Rev. A **60**, 4156 (1999).
[14] D. L. Robbins, A. Ya. Faenov, T. A. Pikuz, H. Chen, P. Beiersdorfer, M. J. May, J. Dunn, K. J. Reed, and A. J. Smith, Phys. Rev. A **70**, 022715-1 (2004).
[15] E. Takács, E. S. Meyer, J. D. Gillaspy, J. R. Roberts, C. T. Chantler, L. T. Hudson, R. D. Deslattes, C. M. Brown, J. M. Laming, J. Dubau, and M. K. Inal, Phys. Rev. A **54**, 1342 (1996).
[16] D. A. Knapp, R. E. Marrs, S. R. Elliott, E. W. Magee, and R. Zasadzinski, Nucl. Instrum. Methods Phys. Res. A **334**, 305 (1993).
[17] P. Beiersdofer, R. E. Marrs, J. R. Henderson, D. A. Knapp, M. A. Levine, D. B. Platt, M. B. Schneider, D. A. Vogel, and K. L. Wong, Rev. Sci. Instrum. **61**, 2338 (1990).
[18] D. L. Robbins, A. Ya. Faenov, T. A. Pikuz, H. Chen, P. Beiersdorfer, M. J. May, J. Dunn, and A. J. Smith, Rev. Sci. Instrum. **75**, 3717 (2004).
[19] B. L. Henke, E. M. Gullikson, and J. C. Davis, At. Data Nucl. Data Tables **54**, 181 (1993).
[20] F. S. Porter, G. V. Brown, K. R. Boyce, R. L. Kelley, C. A. Kilbourne, P. Beiersdorfer, H. Chen, S. Terracol, S. M. Kahn, and A. E. Szymkowiak, Rev. Sci. Instrum. **75**, 3772 (2004).
[21] D. Thorn and P. Beiersdorfer, Rev. Sci. Instrum. **75**, 3937 (2004).
[22] H. L. Zhang, D. H. Sampson, and R. E. H. Clark, Phys. Rev. A **41**, 198 (1990).
[23] F. A. Parpia and W. R. Johnson, Phys. Rev. A **26**, 1142 (1982).
[24] M. F. Gu, P. Beiersdorfer, and D. W. Savin, J. Phys. B **32**, 5371 (1999).
[25] P. Beiersdorfer, R. E. Olson, G. V. Brown, H. Chen, C. L. Harris, P. A. Neill, L. Schweikhard, S. B. Utter, and K. Widmann, Phys. Rev. Lett. **85**, 5090 (2000).
[26] P. Beiersdorfer, R. E. Olson, L. Schweikhard, P. Liebisch, G. V. Brown, J. Crespo López-Urrutia, C. L. Harris, P. A. Neill, S. B. Utter, and K. Widmann, P. Beiersdorfer, R. E. Olson, L. Schweikhard, P. Liebisch, G. V. Brown, J. Crespo López-Urrutia, C. L. Harris, P. A. Neill, S. B. Utter, and K. Widmann, in *The Physics of Electronic and Atomic Collisions*, edited by Y. Itikawa *et al.*, AIP Conf. Proc. No. 500 (AIP, New York, 2000), p. 626.
[27] B. J. Wargelin, P. Beiersdorfer, J. H. Scofield, P. A. Neill, and R. E. Olson, Astrophys. J. **634**, 687 (2005).